Modeling Rectangular Waveguide Junctions by the Eigenfunction Method

ALI H. NALBANDOĞLU, STUDENT MEMBER, IEEE

Abstract—**A method to determine the impedance and admittance matrices of a certain class of rectangular waveguide junctions is presented. First, general matrices are obtained relating all of the modes that may exist in the waveguides connected to the ports. The expressions for the matrix entries are given in terms of the eigenfunctions of the volume occupied by the junction and the fields at the ports. Second, to obtain a relationship between the propagating modes of the connecting waveguides, a numerical iterative procedure is developed to eliminate the evanescent modes from the general matrices. Practical applications have shown that the results agree well with the previous ones, and the method can readily be used to analyze different types of junctions in any required frequency range.**

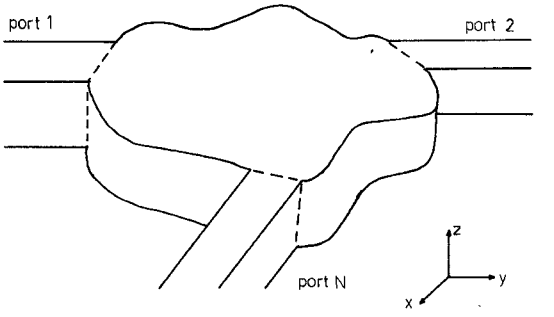

Fig. 1. General form of the rectangular waveguide junctions.

NOMENCLATURE

i	Subscript for layers.
ε_{ri}	Relative permittivity of the ith layer.
d_i	Thickness of the ith layer.
$K(z)$	Relative permittivity function of the junction.
$M(z)$	Relative permeability function of the junction.
$\bar{n}$	Outward normal unit vector.
P plane	The plane perpendicular to the z axis.
p	Subscript for the quantities pertinent to the P plane.
u_1,u_2	Coordinate variables in the P plane.
S_0	Lateral surface occupied by the ports.
S_{ok}	Lateral surface occupied by the kth port.
S_c	Lateral surface not occupied by the ports.
L	Intersection of the P plane and the lateral surface.
L_o	Intersection of the P plane and S_o.
L_{ok}	Intersection of the P plane and S_{ok}.
L_c	Intersection of the P plane and S_c.
$f_m(z),g_m(z)$	Depth eigenfunctions (PM,PE).
D_{em},D_{hm}	Normalization constants for $f_m(z)$ and $g_m(z)$.
γ_m,η_m	Propagation constants in the P plane.
φ_n,ψ_n	Planar eigenfunctions (PM,PE).
λ_n,α_n	Planar eigenvalues (PM,PE).
$\bar{H}_{in},\bar{E}_{in}$	Total (magnetic, electric) fields in the connecting waveguides.

I. INTRODUCTION

A WAVEGUIDE junction can be defined as a closed box filled with a heterogeneous combination of passive material media, connected to the rest of the circuit by closed waveguides through a finite number of clearly definable ports [1]. Early methods developed for their analysis have generally utilized the analytic approach and have been aimed to obtain a formula from which numerical values for a particular set of dimensions may be obtained by hand calculations. A good review of such methods and their applications is given by Marcuvitz [2]. The resulting formulas are all approximate, except for a small group of junctions [3, ch. 10]. However, they served for a long time as an almost unique tool to calculate network parameters, although they need an advanced level of mathematics and apply only to single-mode-propagation cases.

The use of the numerical approach is almost as old as the analytic approach [4], but it became attractive only after the advent of digital computers. Taking the review of Silvester and Csendes [1] and the recent developments into account, one can conclude that numerical methods are more successful in analyzing the single or interacting planar discontinuities. However, special care is required to avoid problems such as relative convergence and inversion of ill-conditioned matrices. Recently there have been studies to eliminate these computational problems [5], however the mathematics employed is quite complicated.

In this paper, a new method is described to model a certain class of rectangular waveguide junctions. The general form of the junctions, shown in Fig. 1, is a cylindrical structure with an arbitrary cross section. It has N ports whose surfaces are planes parallel to the axis of the structure, and whose heights are equal to the height of the structure. Inside the junction there may exist a finite number of layers of lossless media with constant thicknesses and scalar permittivities and permeabilities. The connecting waveguides must have axes perpendicular to the z axis, to make the port surfaces constant-phase planes for the fields. Such a junction generalizes the transversal discontinuities in rectangular waveguides, curves, and ring-type hybrid junctions.

The fields inside the junction are expressed in terms of Hertzian potentials which have only z directed components and can be expanded as a series of the eigenfunctions of the

Manuscript received July 7, 1976; revised December 10, 1976.
The author is with Orta Doğu Teknik Üniversitesi, Elektrik Muhendisliği Bölümü, Ankara, Turkey.

structure. The coefficients in the expansions are determined using the continuity of the tangential fields at the ports. The field analysis is developed in such a manner that the impedance and admittance matrices can easily be obtained using field expressions. The general impedance or admittance matrices are of infinite order and relate all possible modes that may exist in the connecting waveguides. A particular matrix relating only a finite number of modes—usually the propagating modes—can be found from the general matrix by assuming that the electrical ports corresponding to the remaining modes are terminated by their characteristic impedances and eliminating these modes by a numerical procedure.

The eigenfunction expansion of the Hertzian potentials has also been used as a starting point by Ridella and Bianco [6], to analyze transmission-line discontinuities. However, the applications are of limited number and only consider single-mode-propagation cases. Using the eigenfunction expansion method in waveguide-junction analysis results in a method which is applicable to a great number of cases at all frequencies. Furthermore, the simplicity of the required mathematics and programming techniques increases the attractiveness of the method.

II. Field Analysis

As mentioned in the preceding section, all the layers inside the junction have different permittivities and permeabilities and for each layer these parameters are scalar constants. The relative permittivity function $K(z)$ and the relative permeability function $M(z)$ can be given, in the form of piecewise continuous functions, as

$$K(z) = \varepsilon_{ri} \qquad M(z) = \mu_{ri},$$
$$d - \sum_{j=1}^{i} d_j < z < d - \sum_{j=1}^{i-1} d_j \tag{1}$$

where $i = 1, 2, \cdots, n$, and n is the total number of layers.

Since the junction is source free, the fields satisfy the following Maxwell's equations:

$$\nabla \times \bar{H} = j\omega\varepsilon_0 K(z)\bar{E} \tag{2a}$$
$$\nabla \times \bar{E} = -j\omega\mu_0 M(z)\bar{H} \tag{2b}$$
$$\nabla \cdot M(z)\bar{H} = 0 \tag{2c}$$
$$\nabla \cdot K(z)\bar{E} = 0. \tag{2d}$$

Referring to Fig. 1, the junction can be thought of as a piece of cylindrical waveguide of length d, directed along the z axis. Making an analogy to the analysis of cylindrical waveguides [3, ch. 5], the fields in the junction can be divided into two classes. One class will have no H_z component and hence will be called planar magnetic (PM) fields. The other class will have no E_z component and will be called planar electric (PE) fields. In this paper derivations for PM fields are given, and for PE fields only the results are presented.

For PM fields, equation (2c) can be expanded as

$$\nabla \cdot M(z)\bar{H} = \bar{H} \cdot \nabla M(z) + M(z)\nabla \cdot \bar{H} = M(z)\nabla \cdot \bar{H} = 0.$$

Then, due to the definition of PM fields and the shape of the structure, the fields can be derived from the electric Hertzian potential function

$$\bar{A}_e = \bar{a}_z f(z)E_s(u_1,u_2) \tag{3}$$

such that

$$\bar{H} = j\omega\varepsilon_0 \nabla \times \bar{A}_e$$
$$\bar{E} = (\nabla \times \nabla \times \bar{A}_e)/K(z).$$

A procedure similar to the derivations for longitudinal-section magnetic (LSM) modes of inhomogeneously filled waveguides [3, ch. 6] gives the following equations governing $f(z)$ and $E_s(u_1,u_2)$:

$$\frac{d}{dz}\left[\frac{1}{K(z)}\frac{df(z)}{dz}\right] + (K(z)M(z)k_0^2 - \gamma^2)f(z)/K(z) = 0 \tag{4}$$

$$\nabla_p^2 E_s(u_1,u_2) + \gamma^2 E_s(u_1,u_2) = 0 \tag{5}$$

and the following field expressions:

$$\bar{H} = -j\omega\varepsilon_0 f(z)(\bar{a}_z \times \nabla_p E_s(u_1,u_2)) \tag{6}$$
$$\bar{E} = (\bar{a}_z\gamma^2 f(z)E_s(u_1,u_2) + (df(z)/dz)\nabla_p E_s(u_1,u_2))/K(z). \tag{7}$$

As can be noticed, $\bar{H}_p$ is proportional to $f(z)$ and $\bar{E}_p$ is proportional to $(df(z)/dz)/K(z)$, and the continuity of $\bar{H}_p$ and $\bar{E}_p$ at the boundaries between the layers guarantees the continuity of $f(z)$ and $(df(z)/dz)/K(z)$ for all values of z. Thus together with the condition $(df(z)/dz) = 0$ at the top and bottom boundaries, equation (4) becomes a Sturm–Liouville system. Solutions to this type of differential equation have useful properties [7], but for an arbitrary continuous function $K(z)$ it is difficult to obtain closed-form solutions. However, for $K(z)$ given as in (1), equation (4) can be reduced for each layer to the following form:

$$(d^2 f_i(z_i)/dz_i^2) + k_{ci}^2 f_i(z_i) = 0 \tag{8}$$

where the z_i are defined in Fig. 2 and the k_{ci} are given by

$$k_{ci}^2 = \omega^2\varepsilon_0\mu_0\varepsilon_{ri}\mu_{ri} - \gamma^2. \tag{9}$$

The general solution to such an equation is

$$f_i(z_i) = C_{1i} \sin k_{ci}z_i + C_{2i} \cos k_{ci}z_i.$$

The coefficients C_{ji} and the eigenvalues k_{ci} can be determined using the boundary conditions at the top and bottom boundaries and the continuity of the tangential fields at the boundaries between the layers. Straightforward computations lead to a transcendental equation in terms of k_{ci}. For example, for a two-layer junction this equation has the following form:

$$(k_{c1}/\varepsilon_{r1}) \tan k_{c1}d_1 + (k_{c2}/\varepsilon_{r2}) \tan k_{c2}d_2 = 0. \tag{10}$$

Substituting for k_{ci} from (9), the number of unknowns in the transcendental equation reduces to one, namely γ. Due to nature of this equation, there are infinitely many solutions for γ. Each solution γ_m $(m = 0, 1, 2, \cdots, \infty)$ defines a depth eigenfunction $f_m(z)$ which is the sum of $f_{mi}(z_i)$ over all layers. Since the $f_m(z)$ are solutions of (4), they form an orthogonal set of functions, with the orthogonality property defined as

$$\int_0^d (f_m(z)f_n(z)/K(z))\,dz = D_{em}\delta_{mn}.$$

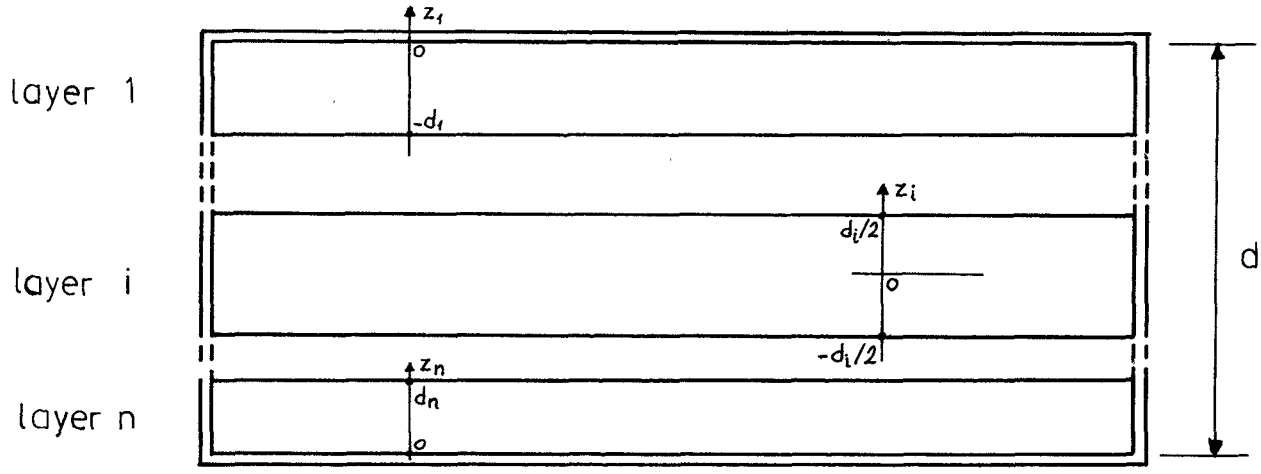

Fig. 2. Coordinate systems used for derivation of the z variation.

Using the above results, equation (5) can be rewritten as

$$\nabla_p^2 E_{sm} + \gamma_m^2 E_{sm} = 0.$$

On the portion of the lateral boundary occupied by the ports, S_o, the boundary conditions for (5) are inhomogeneous and are determined by the fields of incoming waves. On the remaining portion of the lateral boundary, S_c, the boundary conditions imply that E_{sm} must vanish. On S_o either the tangential electric or tangential magnetic field may be specified. If the tangential electric field is specified, the corresponding fields inside the junction are called short-circuit fields; when the tangential magnetic field is specified, the corresponding fields are called open-circuit fields. For a particular junction both open-circuit and short-circuit fields are the same, but the former lead to simpler derivations for the impedance matrix; the latter, for the admittance matrix. The significance of this classification will be clearer in the next section; however, the following intuitive argument can be put forward: For computation of an impedance matrix using network theory, it is general practice to open-circuit all the ports, except one, and to find the mutual impedances. Since a plane on which the tangential magnetic field vanishes is defined as an open-circuited plane in microwave theory, specifying the tangential magnetic fields at the ports is better for computing the impedance matrices.

Thus considering the open-circuit PM fields, the boundary condition for E_{sm} on S_o is determined by the incoming magnetic field. Denoting this field as $\bar{H}_{in}$, and using the continuity of the tangential fields on S_o,

$$\frac{\partial E_{sm}}{\partial n} = \frac{1}{j\omega\varepsilon_0 D_{em}} \int_0^d (f_m(z)/K(z))(\bar{H}_{in} \times \bar{n} \cdot \bar{a}_z)\, dz.$$

Since the boundary conditions are inhomogeneous, E_{sm} can be found using the following expression [7]:

$$E_{sm}(u_1,u_2) = \int_{L_o} G_e(u_1,u_2; u_1',u_2')(\partial E_{sm}/\partial n)\, dL_o'$$

where the Green's function G_e is defined as

$$G_e(u_1,u_2; u_1',u_2') = \sum_{n=1}^{\infty} \varphi_n(u_1,u_2)\varphi_n(u_1',u_2')/(\lambda_n^2 - \gamma_m^2).$$

Defined in Table I, φ_n and λ_n are the planar eigenfunctions and eigenvalues, respectively. Using (3), (6), and (7), $\bar{A}_e$, $\bar{E}$, and $\bar{H}$ can be expressed in terms of the eigenfunctions and the fields at the ports. The expressions for the fields and the eigenfunctions of each class are summarized in Table I. Each term in the series expansions of open-circuit PM and open-circuit PE fields (short-circuit PM and short-circuit PE fields) is defined as a mode, and these modes form a complete set. Thus an arbitrary field inside the junction excited by an arbitrary set of waveguide modes at the ports can be expanded in terms of this set.

III. Network Analysis

To derive the impedance representation, first the port voltages and the port currents are defined. Since all the connecting waveguides are rectangular in shape, there are two orthogonal sets of modes, namely TE and TM modes, present in them. The transverse fields at port k can be expanded in terms of these modes as follows [3, ch. 5]:

$$\bar{E}_{T,k} = \sum_r V_{r,k}\bar{e}_{r,k} \tag{11}$$

$$\bar{H}_{T,k} = \sum_r I_{r,k}\bar{h}_{r,k}. \tag{12}$$

The summations cover all TE and TM modes present in the connecting waveguide. $\bar{e}_{r,k}$ and $\bar{h}_{r,k}$ are mode functions related by

$$\bar{h}_{r,k} = \bar{n} \times \bar{e}_{r,k}$$

and normalized as

$$\int_{S_{ok}} \bar{e}_{r,k} \times \bar{h}_{r,k} \cdot \bar{n}\, dS_{ok} = 1.$$

$V_{r,k}$ and $I_{r,k}$ are the voltage and the current corresponding to mode r at port k. From (11) any port voltage can be obtained by

$$V_{r,k} = (\bar{E}_k,\bar{e}_{r,k})_k = (\bar{E}_{T,k},\bar{e}_{r,k})_k = \int_{S_{ok}} (\bar{E}_{T,k} \cdot \bar{e}_{r,k})\, dS_{ok}. \tag{13}$$

TABLE I
EXPRESSIONS FOR THE EXPANSIONS OF THE FIELDS INSIDE THE JUNCTION

	PM modes		PE modes	
Field Expressions	$\bar{H} = \sum_n \sum_m A_{nm} f_m(z)\,(\bar{a}_z \times \nabla_p \psi_n)$ $\bar{E} = \sum_n \sum_m \frac{A_{nm}}{j\omega\epsilon_0 K(z)}\,(\bar{a}_z \gamma_m^2 f_m(z)\psi_n + \frac{df_m(z)}{dz}\nabla_p \psi_n)$		$\bar{E} = \sum_n \sum_m B_{nm} g_m(z)\,(\bar{a}_z \times \nabla_p \psi_n)$ $\bar{H} = \sum_n \sum_m \frac{B_{nm}}{j\omega\mu_0 M(z)}\,(\bar{a}_z \eta_m^2 g_m(z)\psi_n + \frac{dg_m(z)}{dz}\nabla_p \psi_n)$	
Depth Eigenfunc.	$\frac{d}{dz}\left[\frac{1}{K(z)}\frac{df_m(z)}{dz}\right] + (k_0^2 M(z) - \gamma_m^2/K(z))f_m(z) = 0$ $df_m(z)/dz = 0 \quad$ at $z = 0, d$		$\frac{d}{dz}\left[\frac{1}{M(z)}\frac{dg_m(z)}{dz}\right] + (k_0^2 K(z) - \eta_m^2/M(z))g_m(z) = 0$ $g_m(z) = 0 \quad$ at $z = 0, d$	
	Open circuit PM modes	Short circuit PM modes	Open circuit PE modes	Short circuit PE modes
Planar Eigenfunc.	$\nabla_p^2 \psi_n + \lambda_n^2 \psi_n = 0$ $\partial\psi_n/\partial n = 0 \quad$ on L_o $\psi_n = 0 \quad$ on L_c	$\nabla_p^2 \psi_n + \lambda_n^2 \psi_n = 0$ $\psi_n = 0 \quad$ on L_o and L_c	$\nabla_p^2 \psi_n + \alpha_n^2 \psi_n = 0$ $\psi_n = 0 \quad$ on L_o $\partial\psi_n/\partial n = 0 \quad$ on L_c	$\nabla_p^2 \psi_n + \alpha_n^2 \psi_n = 0$ $\partial\psi_n/\partial n = 0 \quad$ on L_o and L_c
Coefficients	$A_{nm} = \frac{1}{D_{em}(\lambda_n^2 - \gamma_m^2)} \cdot \int_{S_o} \psi_n \frac{f_m(z)}{K(z)}\,(\bar{n} \times \bar{H}_{in} \cdot \bar{a}_z)\,dS_o$	$A_{nm} = \frac{j\omega\epsilon_0}{D_{em}\gamma_m^2(\lambda_n^2 - \gamma_m^2)} \cdot \int_{S_o} \frac{\partial\psi_n}{\partial n} f_m(z)\,(\bar{E}_{in} \cdot \bar{a}_z)\,dS_o$	$B_{nm} = \frac{-j\omega\mu_0}{D_{hm}\eta_m^2(\alpha_n^2 - \eta_m^2)} \cdot \int_{S_o} \frac{\partial\psi_n}{\partial n} g_m(z)\,(\bar{H}_{in} \cdot \bar{a}_z)\,dS_o$	$B_{nm} = \frac{1}{D_{hm}(\alpha_n^2 - \eta_m^2)} \cdot \int_{S_o} \psi_n \frac{g_m(z)}{M(z)}\,(\bar{n} \times \bar{E}_{in} \cdot \bar{a}_z)\,dS_o$

Note that using the total field $\bar{E}_k$ or the tangential field $\bar{E}_{T,k}$ does not make any difference, since $\bar{e}_{r,k}$ is already tangential to the port surface.

As it was mentioned before, the open-circuit field expressions will be used in the derivation of the impedance matrix. From Table I, the total electric field (both PM and PE modes) can be written as

$$\begin{aligned}\bar{E}_k = \sum_m \sum_n & - A_{nm}(\bar{a}_z \gamma_m^2 f_m(z)\varphi_n \\ & + (df_m(z)/dz)\nabla_p \varphi_n)/j\omega\varepsilon_0 K(z) \\ & + B_{nm} g_m(z)(\bar{a}_z \times \nabla_p \psi_n). \end{aligned} \tag{14}$$

Referring to (12), the total magnetic field of the incoming waves, $\bar{H}_{in}$, can be expressed as

$$\bar{H}_{in} = \sum_{j=1}^{N} \sum_s I_{s,j} \bar{h}_{s,j}$$

where the first summation is over the ports and the second is over the TE and/or the TM modes. Then the coefficients A_{nm} and B_{nm} become

$$A_{nm} = -a_{nm} \sum_{j=1}^{N} \sum_s I_{s,j}(\bar{e}_{s,j}\bar{a}_z f_m(z)\varphi_n/K(z))_j \tag{15}$$

$$B_{nm} = b_{nm} \sum_{j=1}^{N} \sum_s I_{s,j}(\bar{e}_{s,j} g_m(z)(\bar{a}_z \times \nabla_p \psi_n))_j. \tag{16}$$

a_{nm} and b_{nm} can be found by comparing the above expressions with the ones in Table I. Substituting (14)–(16) into (13), the voltage $V_{r,k}$ can be expressed as

$$V_{r,k} = \sum_{j=1}^{N} \sum_s Z_{rk,sj} I_{s,j} \tag{17}$$

where

$$\begin{aligned} Z_{rk,sj} = \sum_{m=1}^{\infty} \sum_{n=1}^{\infty} & \frac{a_{nm}\gamma_m^2}{j\omega\varepsilon_0}\left(\bar{a}_z \frac{f_m(z)\varphi_n}{K(z)}, \bar{e}_{s,j}\right)_j \\ & \cdot \left(\bar{a}_z \frac{f_m(z)\varphi_n}{K(z)}, \bar{e}_{r,k}\right)_k \\ & + \frac{a_{nm}}{j\omega\varepsilon_0}\left(\bar{a}_z \frac{f_m(z)\varphi_n}{K(z)}, \bar{e}_{s,j}\right)_j \\ & \cdot \left(\frac{df_m(z)/dz}{K(z)}\nabla_p \varphi_n, \bar{e}_{r,k}\right)_k \\ & + b_{nm}(\bar{a}_z \times \nabla_p \psi_n g_m(z), \bar{e}_{s,j})_j \\ & \cdot (\bar{a}_z \times \nabla_p \psi_n g_m(z), \bar{e}_{r,k})_k \end{aligned} \tag{18}$$

is the mutual impedance between the rth mode at port k and the sth mode at port j. Repeating the above procedure for each port voltage, the results can be written in matrix form as

$$\begin{bmatrix} V_1 \\ V_2 \\ \vdots \\ V_N \end{bmatrix} = \begin{bmatrix} Z_{11} & Z_{12} & \cdots & Z_{1N} \\ Z_{21} & Z_{22} & \cdots & Z_{2N} \\ \vdots & \vdots & & \vdots \\ Z_{N1} & Z_{N2} & \cdots & Z_{NN} \end{bmatrix} \begin{bmatrix} I_1 \\ I_2 \\ \vdots \\ I_N \end{bmatrix} \tag{19}$$

where $I_k = [I_{i,k}]$ and $V_k = [V_{i,k}]$ $(i = 1, 2, \cdots, \infty)$ are the current and voltage vectors of port k, respectively.

At this stage, the idea behind the eigenfunction method can be explained. In the preceding section, the fields inside the junction were found in terms of the PM and PE modes defined by the eigenfunctions. The amplitudes of the modes,

denoted by A_{nm} and B_{nm} were determined by the fields at the ports. In view of the expressions obtained for A_{nm} and B_{nm} in (15) and (16), the amplitudes of the junction modes can be considered as the sum of the contributions from each port current. Substitution of (14) into (13) shows that every port voltage is the sum of the contributions from each junction mode. Therefore, it can be concluded that the port voltages can be written as a weighted sum of port currents. The weighting factors are defined as the mutual impedances and are given in (18). Thus without computing the amplitudes of the junction modes, the port voltages and currents are related with each other, to form an impedance representation.

A similar derivation gives an admittance representation, which is the dual of (19), where the entries are given by

$$\begin{aligned} Y_{rk,sj} = \sum_{m=1}^{\infty}\sum_{n=1}^{\infty} & c_{nm}(\bar{a}_z \times \nabla_p \varphi_n\, f_m(z), \bar{h}_{s,j})_j \\ & \cdot (\bar{a}_z \times \nabla_p \varphi_n\, f_m(z), \bar{h}_{r,k})_k \\ & + \frac{d_{nm}\eta_m^2}{j\omega\mu_0}\left(\bar{a}_z \frac{g_m(z)\psi_n}{M(z)}, \bar{h}_{s,j}\right)_j \\ & \cdot \left(\bar{a}_z \frac{g_m(z)\psi_n}{M(z)}, \bar{h}_{r,k}\right)_k \\ & + \frac{d_{nm}}{j\omega\mu_0}\left(\bar{a}_z \frac{g_m(z)\psi_n}{M(z)}, \bar{h}_{s,j}\right)_j \\ & \cdot \left(\frac{dg_m(z)/dz}{M(z)} \nabla_p \psi_n, \bar{h}_{r,k}\right)_k . \end{aligned}$$

The impedance matrix given in (19) is of infinite order and in general covers all the TE and TM modes in the connecting waveguides. In practice, there will be no need to consider all the modes for a particular case, and the fields at the ports can be approximated by the propagating modes plus a finite number of evanescent modes. Then the impedance matrix will be of finite order, but still some manipulations will have to be made to eliminate the voltages and currents corresponding to evanescent modes.

Although the junction has N physical ports, the number of electrical ports is greater than N. In fact it is equal to the sum of all the modes that are used to approximate the fields at the ports. In the electrical ports corresponding to evanescent modes, these modes appear only as reflected waves, in other words, as propagating in one direction. If the connecting waveguides are sufficiently long, the electrical ports corresponding to the evanescent mode p at port q can be thought of as terminated by a matched load or the wave impedance $Z_{p,q}$. Such a condition implies that the voltage and current of this mode can be eliminated from the impedance matrix, by defining a new matrix whose entries are given by

$$Z'_{rk,sj} = Z_{rk,sj} - \frac{Z_{rk,pq}Z_{pq,sj}}{Z_{pq,pq} + Z_{p,q}} \tag{20}$$

and deleting the row corresponding to $V_{p,q}$ and the column corresponding to $I_{p,q}$ from the new matrix [8]. Repeating this for all evanescent modes, a particular matrix is obtained relating only the propagating modes in the connecting waveguides. The resulting matrix is approximate, and the exact matrix can be obtained when the fields are approximated by infinitely many modes. However, the above procedure is a converging one, and quite accurate results can be obtained by using a finite number of evanescent modes.

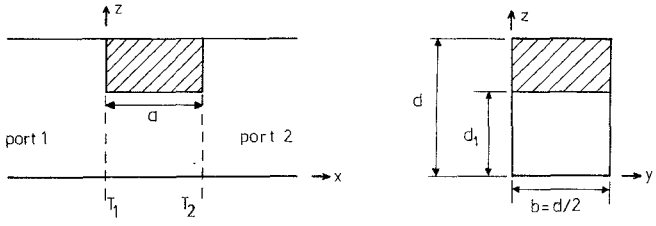

Fig. 3. Side and front views of thick asymmetrical inductive window.

IV. An Example

To illustrate the application of the theory, the impedance matrix for the asymmetrical inductive window, shown in Fig. 3, is computed. The first layer of the junction is a perfect conductor, and the second layer is air. It is assumed that the frequency range is such that only an H_{10} mode can propagate in the connecting waveguides. Since the junction has no y variation, only H_{n0} modes will be excited, for which the mode functions are

$$\bar{e}_{r,1} = \bar{e}_{r,2} = \bar{a}_y\sqrt{2/bd}\,\sin(r\pi z/d) \tag{21a}$$

$$\bar{h}_{r,1} = -h_{r,2} = \bar{a}_z\sqrt{2/bd}\,\sin(r\pi z/d). \tag{21b}$$

Since the fields at the ports have no E_z components, only PE modes are excited in the junction, and the corresponding eigenfunctions and eigenvalues can be summarized as

$$\begin{aligned} g_m(z) &= \sqrt{2/d_1}\,\sin(m\pi z/d_1) \qquad \eta_m^2 = k_o^2 - (m\pi/d_1)^2 \\ \psi_{qn} &= \sqrt{2\varepsilon_{oq}/ab}\,\cos(q\pi y/b)\,\sin(n\pi x/a) \\ \alpha_{qn}^2 &= (n\pi/a)^2 + (q\pi/b)^2 \end{aligned} \tag{22}$$

where ε_{oq} is the Neumann factor and equals unity for $n = 0$, and 2 otherwise. Substituting (21) and (22) into (18), the entries of the impedance matrix are found as

$$Z_{11}(r,s) = Z_{22}(r,s) = -j\omega\mu_0(4d_1/\pi^2 d)\,\sin(r\pi d_1/d)\,\sin(s\pi d_1/d)$$

$$\cdot \sum_{m=1}^{\infty} \frac{m^2 \cot\left(a(k_0^2 - (m\pi/d_1)^2)^{1/2}\right)}{(k_0^2 - (m\pi/d_1)^2)^{1/2}(m^2 - (sd_1/d)^2)(m^2 - (rd_1/d)^2)}.$$

TABLE II
VARIATION OF NETWORK PARAMETERS WITH NUMBER OF APPROXIMATING MODES

q	$\bar{Z}_{11}$	$\bar{Z}_{12}$
1	j 0.2420	j 1.1210
3	j 0.2176	j 1.1139
5	j 0.2040	j 1.1065
7	j 0.1976	j 1.1023
9	j 0.1963	j 1.1013
11	j 0.1962	j 1.1012
13	j 0.1959	j 1.1011
15	j 0.1951	j 1.1006
17	j 0.1943	j 1.1000
19	j 0.1940	j 1.0999
20	j 0.1940	j 1.0998
Dimensions : a = 20 cm , d = 2 cm , $d_1 = 0.9d$		
Frequency : 11 GHz		

For $Z_{12}(r,s)$ and $Z_{21}(r,s)$, the cotangent will be replaced by the cosecant in the above expression.

A computer program has been prepared to compute the matrix entries and then to eliminate the evanescent modes by using (20). The fields at the ports are approximated by the fundamental mode and q higher modes. Changing q, the frequency, and the dimensions of the junction, the parameters for a number of cases are calculated.

First, the convergence of the procedure used to eliminate the evanescent modes is investigated. The results for a particular set of dimensions with a different number of approximating modes are given in Table II. The convergence error is found to be less than 0.1 percent for this case, and less than 1 percent in all other cases, with the maximum value of q being 20. Also, the convergence error is around 0.5 percent for $q = 11$, which is acceptable for many applications. Thus to have a small computer-program size and reasonable accuracy, it is sufficient to use about ten higher modes to approximate the fields at the ports.

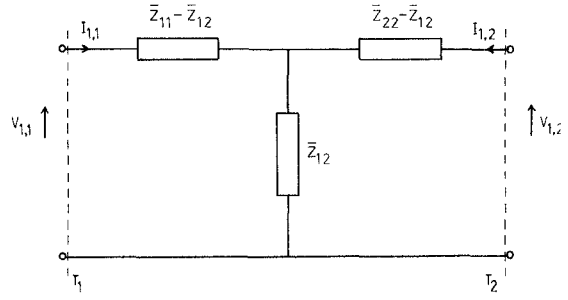

Fig. 4. T-network representation for the asymmetrical inductive window.

In the second step q is set equal to 9, and the network parameters are calculated for various sets of dimensions and frequency. The results, together with the ones obtained from the formulas of Marcuvitz [2, sec. 8–9], are given in Table III. The conventional T-network representation of the junction is shown in Fig. 4. All the impedance values are normalized with respect to the wave impedance of the H_{10} mode. The variations of the parameters are similar in both cases and the numeric values differ only with an error of less than 5 percent, except for a few cases. Since both the eigenfunction method and the formulas of Marcuvitz are approximate, these errors can be tolerated. For the cases with high discrepancies in the numerical values, it is observed that the results are affected to a great extent by the reading errors on the graphs given by Marcuvitz.

TABLE III
VARIATION OF THE NETWORK PARAMETERS WITH FREQUENCY AND DIMENSIONS (d = 2 cm)

		a = 20 cm				a = 2 cm			
		$\bar{Z}_{11} - \bar{Z}_{12}$		$\bar{Z}_{12}$		$\bar{Z}_{11} - \bar{Z}_{12}$		$\bar{Z}_{12}$	
f	d_1/d	Numeric	Theoretic	Numeric	Theoretic	Numeric	Theoretic	Numeric	Theoretic
8 GHz	0.2	j 0.0	j 0.001	j 0.0	j 0.0	j 0.0	j 0.001	j 0.0	j 0.0
	0.5	j 0.055	j 0.056	j 0.0	j 0.0	j 0.055	j 0.056	j 0.0	j 0.0
	0.75	j 0.281	j 0.279	j 0.0	j 0.0	j 0.251	j 0.248	j 0.031	j 0.031
	0.9	j 0.978	j 0.977	j 0.0	j 0.0	j 0.489	j 0.487	j 0.653	j 0.635
11 GHz	0.2	j 0.001	j 0.005	j 0.0	j 0.0	j 0.001	j 0.005	j 0.0	j 0.0
	0.5	j 0.189	j 0.201	j 0.0	j 0.0	j 0.186	j 0.197	j 0.003	j 0.003
	0.75	j 0.257	j 0.253	j 2.476	j 3.549	j 1.281	j 1.355	-j 1.378	-j 1.344
	0.9	-j 0.905	-j 0.913	j 1.101	j 1.104	j 8.730	j 8.432	-j 4.398	-j 4.220
14 GHz	0.2	j 0.002	j 0.007	j 0.0	j 0.0	j 0.002	j 0.007	j 0.0	j 0.0
	0.5	j 0.456	j 0.455	j 0.0	j 0.0	j 0.410	j 0.408	j 0.046	j 0.047
	0.75	j37.314	j92.942	-j18.590	-j46.410	-j 2.429	-j 2.309	j 1.471	j 1.405
	0.9	j 34.416	j29.411	-j17.202	-j14.701	-j 1.039	-j 1.062	j 1.024	j 1.034

The best criteria for verifying the method are the experimental results; the investigations are in progress. Nevertheless, it is apparent from the above discussion that quite accurate results can be obtained by the eigenfunction method employing a small number of evanescent modes.

V. Conclusion

Starting from eigenfunction expansion of the fields inside the junction, a procedure to determine the impedance and admittance representations of a certain class of rectangular waveguides has been developed. The derivation of the expressions for the matrix entries is straightforward once the eigenfunctions of the junction are found. When the lateral boundaries of the junction coincide with the constant coordinate surfaces of a cylindrical coordinate system, closed-form expressions can be obtained for the eigenfunctions. However, for junctions with arbitrary cross sections, numerical methods have to be used to obtain approximate eigenfunctions. For many practical cases the eigenfunctions are in the form of the trigonometric and/or the Bessel's function and can easily be used in appropriate expressions.

One of the features of the method is that it can be used at any frequency. This is because matrices covering all the modes in the connecting waveguides are found at the beginning, and then at a given frequency the evanescent modes are eliminated, giving a relation between the propagating modes which may be of any number.

Since it is required that all the ports must be on the lateral boundary, devices such as the magic-T cannot be analyzed. Also, for computations to be simple, the heights of the connecting waveguides must be the same as the junction height.

Acknowledgment

The author wishes to thank Assoc. Prof. Dr. C. Toker for his valuable comments and discussions during this work. He also wishes to thank Dr. Y. Ayasli for his constructive suggestions in the preparation of this manuscript.

References

[1] P. Silvester and Z. J. Csendes, "Numerical modeling of passive devices," *IEEE Trans. Microwave Theory Tech.*, vol. MTT-22, pp. 190–201, Mar. 1974.
[2] N. Marcuvitz, *Waveguide Handbook*. New York: McGraw-Hill, 1951.
[3] R. E. Collin, *Field Theory of Guided Waves*. New York: McGraw-Hill, 1960.
[4] J. R. Whinnery and H. W. Jamieson, "Equivalent circuits for discontinuities in transmission lines," *Proc. IRE*, vol. 32, pp. 98–114, Feb. 1944.
[5] T. E. Rozzi, "The variational treatment of thick interacting inductive irises," *IEEE Trans. Microwave Theory Tech.*, vol. MTT-21, pp. 82–88, Feb. 1973.
[6] S. Ridella and B. Bianco, "Nonconventional transmission zeros in distributed rectangular structures," *IEEE Trans. Microwave Theory Tech.*, vol. MTT-20, pp. 297–303, May 1972.
[7] P. M. Morse and H. Feshbach, *Methods of Theoretical Physics*, Part I. New York: McGraw-Hill, 1953, ch. 6–7.
[8] C. G. Montgomery, R. H. Dicke, and E. M. Purcell, *Principles of Microwave Circuits*. New York: McGraw-Hill, 1948, p. 127.

High-Efficiency Millimeter-Wave Bolometer Mount

TAKEMI INOUE, MEMBER, IEEE, AND TOSHIO NEMOTO, MEMBER, IEEE

Abstract—**A bolometer mount is described for measuring TE_{01}-mode waveguide power at a frequency of 100 GHz. This device is called an eight-fan-type bolometer mount. By dividing the electrode of the element into eight segments, the generation of an unwanted mode was suppressed, and, by minimizing the electrode area, heat loss due to the electrode was decreased.**

As a result, good matching characteristics and high effective efficiency were obtained. This mount is sufficiently useful for a precision power measurement in the millimeter-wave region.

Introduction

A BOLOMETER MOUNT is a standard device for measuring power at both centimeter and millimeter wavelengths. As the frequency increases in the millimeter-wave region, it becomes difficult to make a bolometer mount with good performances.

An effective efficiency [1] is obtained on bolometer mounts; effective efficiency is the ratio of the substituted bias power to the net RF power input to the bolometer mount. The effective efficiency generally degrades with increasing frequency in the millimeter wavelengths. This is so mainly because the millimeter-wave power dissipated in places other than the detecting element increases in the mount, and because the difference in the effectiveness of the millimeter-wave and the bias power in the element increases, owing to the expansion of the relative relation between the dimension of the bolometer element and that of the wavelength.

For instance, there is a commercially available thermistor mount having an efficiency of about 60 percent [2]. This efficiency is much lower than that of a conventional bolometer mount in the centimeter-wave region. A bolometer

Manuscript received July 12, 1976; revised January 18, 1977.
The authors are with the Radioelectronics Section, Opto & Radioelectronics Division, Electrotechnical Laboratory, 5-4-1 Mukodai-machi, Tanashi, Tokyo, Japan.